# One-step formation of multiple emulsions in microfluidics†

Adam R. Abate,‡[a] Julian Thiele‡[ab] and David A. Weitz*[a]

*Received 23rd July 2010, Accepted 21st September 2010*
**DOI: 10.1039/c0lc00236d**

We present a robust way to create multiple emulsions with controllable shell thicknesses that can vary over a wide range. We use a microfluidic device to create a coaxial jet of immiscible fluids; using a dripping instability, we break the jet into multiple emulsions. By controlling the thickness of each layer of the jet, we adjust the thicknesses of the shells of the multiple emulsions. The same method is also effective in creating monodisperse emulsions from fluids that cannot otherwise be controllably emulsified, such as, for example, viscoelastic fluids.



## Introduction

Multiple emulsions are drops containing smaller drops within them.[1–3] They are useful for making particles and capsules through a templating process.[4–6] Multiple emulsions can be formed with the desired structure using microfluidic devices;[7–9] by solidifying the drops, they can be transformed into particles or capsules whose properties are determined by those of the multiple emulsions. These capsules are useful because they provide a protective shell for active reagents; by tuning the properties of the shell, the capsules can be triggered to burst, to release their payloads under specific conditions of heat, pH, or physical stresses.[2,10,11] This makes capsules formed with microfluidics valuable for a range of active delivery applications, including for fragrances and enhancing enzymes in cosmetics, pharmaceuticals, and the controlled release of pesticides.[12–15] However, current microfluidic techniques are limited because drops can be formed only with a narrow range of shell thicknesses. This limitation arises due to the mechanism of formation: In the best approach, the drops are formed by a multi-step mechanism; a series of drop makers are aligned end-to-end such that the output of one feeds the input of the next. Thus, the innermost drop is formed in the first drop maker and encapsulated in drops of increasing size in the next drop makers, producing the multiple emulsion in a stepwise process.[16,17] For example, to create a triple emulsion, the innermost drop is encapsulated in a larger drop to form a double emulsion, which is then encapsulated in a still larger drop to produce the triple emulsion. To produce monodisperse emulsions, the flow rates must be set to ensure that all junctions operate in the dripping regime.[18] This is the regime in which monodisperse drops are formed at a periodic rate at a fixed location in the device. This limits the flow rates to a narrow range, and typically results in multiple emulsions with thick shells. However, many applications demand much thinner shells. Thus, a versatile method that can operate over a wide range of flow rates is essential.

In this paper we present a simple and robust technique to form multiple emulsions with a wide range of shell thicknesses. We use a microfluidic device consisting of a series of flow-focus junctions. By setting the flow rates such that all but the final junction are in the jetting regime, we produce a coaxial multiple jet of the fluids. The jet itself is broken into multiple emulsions using a dripping instability; a dripping instability is one in which a confined jet is broken into monodisperse drops at a periodic rate at a fixed location in the channel. This mechanism can thus operate at flow rates in which the inner phase is jetting, enabling production of multiple emulsions with a wider range of shell thicknesses. It can also create monodisperse drops from fluids that normally cannot be emulsified controllably, such as viscoelastic fluids. This is achieved by surrounding the viscoelastic fluid in a second fluid that is easier to emulsify; by inducing the outer fluid to pinch into drops, we also pinch the inner fluid into drops. The inner drops can be released by breaking the double emulsions, yielding a monodisperse emulsion of the viscoelastic fluid.

## Results and discussion

We create our emulsions using a flow-focusing geometry, which consists of two channels that intersect to form a cross.[19,20] The dispersed phase is injected into the central inlet and the continuous phase into the side inlets. The fluids meet in the nozzle where drops are formed over a wide range of flow conditions, which can be described by two dimensionless numbers. The Weber number of the dispersed phase $We_{in} = \rho v_{in}^2 l/\gamma$ relates the magnitude of inertial forces to surface forces; $\rho$ and $v_{in}$ are the density and velocity of the inner phase, $l$ the diameter of the channel, and $\gamma$ the surface tension of the jet.[21] The Capillary number of the outer phase $Ca_{out} = \mu v_{out}/\gamma$ relates the magnitude of the shear on the jet, due to the continuous phase, to its surface tension; $\mu$ and $v_{out}$ are the viscosity and velocity of the outer phase.[22] For $\{We_{in}, Ca_{out}\} > 1$, the dispersed phase does not break into drops, whereas for $\{We_{in}, Ca_{out}\} < 1$, a dripping instability occurs, breaking the dispersed phase into drops. Drop formation in microfluidics is usually classified as being shear dominated or pressure dominated. Shear dominated formation tends to occur in unconfined geometries, in which $Ca \approx 1$,[23] whereas pressure dominated drop formation occurs in confined geometries in which $Ca < 0.01$. In our system, $Ca > 0.01$, but the

[a]*School of Engineering and Applied Sciences/Department of Physics, Harvard University, Cambridge, Massachusetts, USA. E-mail: weitz@seas.harvard.edu; Tel: +1-617-495-3275*
[b]*Institute of Physical Chemistry, University of Hamburg, Germany*

† Electronic supplementary information (ESI) available: Movies of one-step double and triple emulsion formation. See DOI: 10.1039/c0lc00236d

‡ Both authors contributed equally to this work.

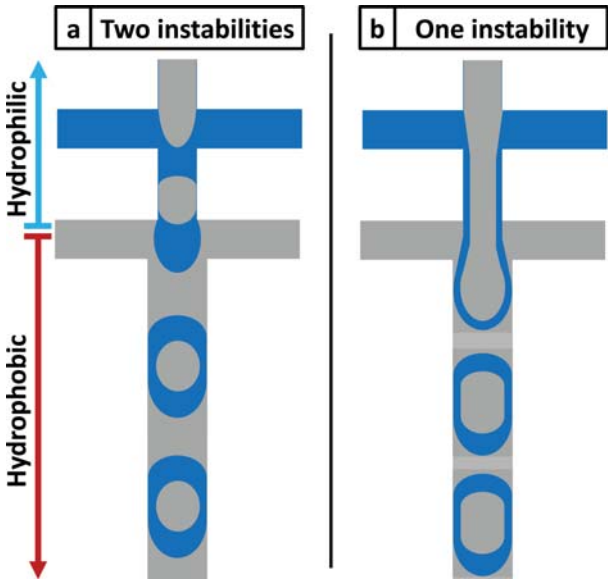


**Fig. 1** (a) Schematic of a double flow-focus device for double emulsion formation. The flow rates are normally set so that dripping instabilities are present in both junctions; this emulsifies the inner phase and then the outer phase, producing double emulsions in a two-step process. (b) By increasing flow rates the first instability can be removed, causing the inner phase to jet; this forms a double jet that can be broken into double emulsions in one step.

flows are confined, precluding direct application of either formalism. Rather, in our system, the drop formation mechanism likely combines shear and pressure effects.

When forming double emulsions, two flow-focus junctions are used; the outlet of the first feeds the inlet of the next, as shown in Fig. 1a. Normally, dripping instabilities are present in both junctions. This produces double emulsions in a two-step process: the inner drop is formed in the first junction and encapsulated in the outer drop in the second.[18,24–26]

Double emulsions can also be formed in a one-step process by removing the first dripping instability, by increasing the flow rates in the first junction. This produces a jet of the inner phase that extends into the second junction. There, it is surrounded by a sheath of middle phase, producing a coaxial jet, as illustrated in Fig. 1b. If the flow rates in the second junction are set to induce a dripping instability, the coaxial jet is pinched into double emulsions, as depicted in Fig. 1b. Thus, there are two distinct types of double emulsification: in two-step formation there are two regions in which drops are formed, whereas in one-step formation all drops form in a single region.

To demonstrate control over the formation process using dripping instabilities, we construct a double flow-focus device with a constant channel height of 50 μm. The width of the nozzle channel in the first junction is 50 μm and in the second junction 80 μm. For the fluids, we use deionized water with sodium dodecyl sulfate (SDS) at 0.5% by weight, and HFE-7500 fluorocarbon oil with the ammonium carboxylate of Krytox® 157 FSL at 1.8% by weight as the surfactant. The density is

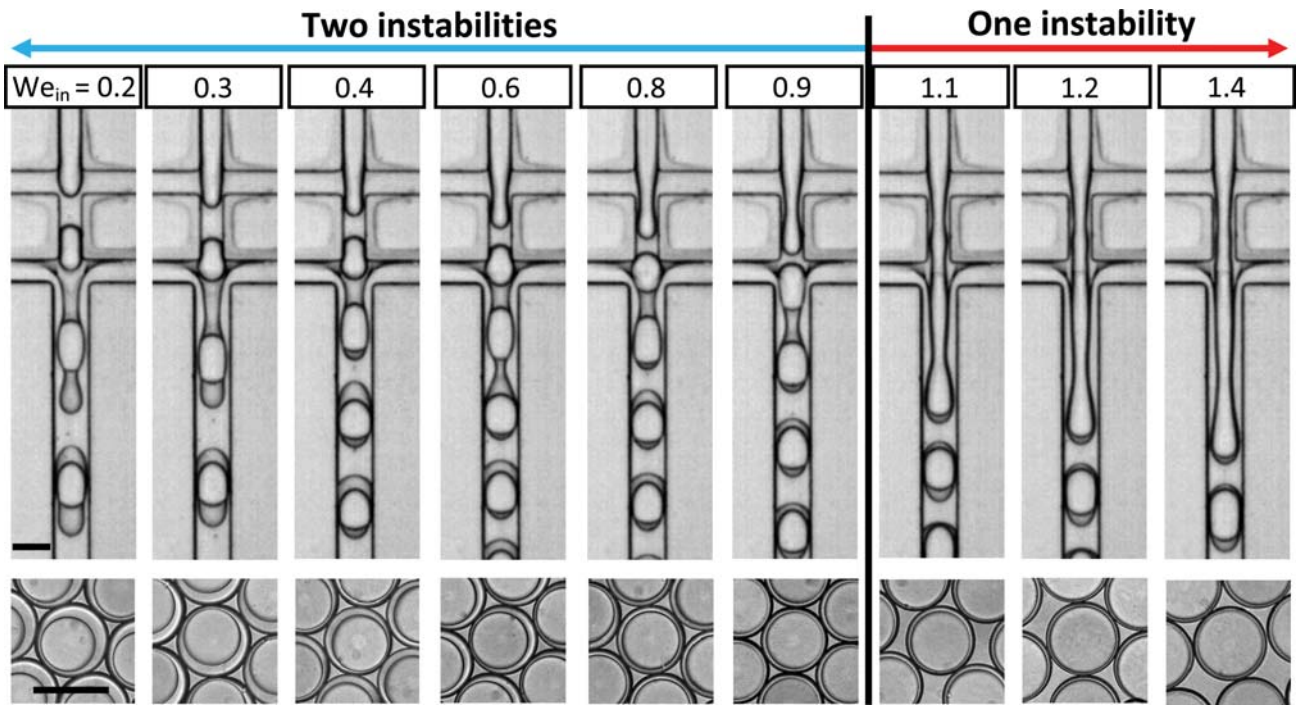


**Fig. 2** Double emulsion formation for different inner-phase Weber numbers, We$_{in}$. For low We$_{in}$, dripping instabilities are present in both junctions, forming double emulsions in a two-step process. When We$_{in}$ is increased beyond one, the first instability is removed; this causes the inner phase to jet, forming a double jet that breaks in a one-step pinch off. The inner and continuous phases, injected into the first and third inlets, are composed of HFE-7500 with the ammonium salt of Krytox® FSL at 1.8% by weight; the middle phase, injected into the second inlet, is water with sodium dodecyl sulfate (SDS) at 0.5% by weight. The scale bars denote 80 μm.



 

1614 kg $m^{-3}$ for HFE 7500 and 998.3 kg $m^{-3}$ for water. The viscosity is 0.77 cSt for HFE 7500 and 1.01 cSt for water. We estimate the surface tension between the dispersed and continuous phase to be 1–5 mN $m^{-1}$. To form O/W/O double emulsions, we pattern the wettability of the device such that the first junction is hydrophilic and the second hydrophobic. We accomplish the patterning of the wettability using a flow-confinement technique.[27] Wettability patterning is needed for both two-step and one-step formation. In two-step formation it is necessary to form the inner and outer drops in two different junctions. In one-step formation, it is necessary to form the coaxial jets that are broken into double emulsions. An advantage with one-step formation is that the patterning does not have to be as precise as with two-step formation. This is because once the inner jet is formed it is surrounded by a protective sheath of the middle phase; this allows it to remain encapsulated even if the channel properties in that region favor wetting. This makes one-step formation easier to implement and, generally, more robust in practice.

We begin by forming double emulsions with the two-step process. This requires two dripping instabilities, one in each junction. We set flow rates to 600 μL $h^{-1}$ for the inner, 1000 μL $h^{-1}$ for the middle, and 2500 μL $h^{-1}$ for the continuous phase, ensuring that $\{We_{in}, Ca_{out}\} < 1$ in both junctions. This causes the innermost phase to drip in the first junction, and the middle phase to drip in the second, forming double emulsions in a two-step process, as shown for $We_{in} = 0.2$ in Fig. 2. As we increase $We_{in}$, the first flow-focus junction approaches the jetting transition, although the process remains two-step, as shown for $We_{in} = 0.8$ in Fig. 2. As we increase $We_{in}$ above 1, the inner phase begins to jet, producing a coaxial jet, as shown for $We_{in} = 1.1$ in Fig. 2. Because $\{We_{in}, Ca_{out}\} < 1$ in the second junction, a dripping instability breaks the coaxial jet into double emulsions, as shown in Fig. 2.

To quantify the transition between these formation processes, we measure the pinch-off locations of the drops. At low $We_{in}$, the inner and middle phases pinch off at different locations, because there are two separated dripping instabilities, as shown in Fig. 3a. As $We_{in}$ is increased, both pinch-offs are displaced downstream due to the higher shear, though the process remains two-step, as shown in Fig. 3a. As $We_{in}$ is increased beyond 1, the inner phase jets; the drops pinch off at the same place, as shown in Fig. 3a. The transition is sudden, due to the discontinuous nature of the dripping-to-jetting transition.[28–30] As the ratio of innermost to middle phase fluids increases, the shell thicknesses decrease, as shown in Fig. 3b. We measure the average shell thickness $T$ by computing the difference in the radii of the outer and inner drops, measured optically. With two-step formation, shells thinner than 7 μm cannot be formed because the requisite flow conditions do not allow dripping; by contrast, with one-step formation we operate in the jetting regime, producing double emulsions with thin shells, as shown in Fig. 3b. To obtain the function for $T$, we equate the shell volume to the volume of middle phase supplied over a single drop cycle; this produces a function that depends only on $We_{in}$ and the known constants, $r_{in}$ the inner drop radius measured from the images, and $a$, a parameter equal to the product of known constants; the function is plotted with the data without free fitting parameters, as shown in Fig. 3b. The precision of the shell thickness measurement is limited by our ability to resolve the droplet interfaces, which for our images is ~1 μm.

To visualize the dynamics of one-step formation, we record movies with a high-speed camera. Early in the cycle, the coaxial jet extends into the flow-focus junction, as shown for $t = 0$ μs in Fig. 4. This allows the dripping instability to narrow the coaxial jet. Since the inner jet is thinner than the outer jet, it reaches an unstable width sooner; this causes it to pinch into a drop before the outer jet, as shown for $t = 375$ μs. As the cycle progresses the outer jet continues to narrow and ultimately breaks, producing the double emulsion at $t = 625$ μs.

One-step formation can also be used to create higher-order multiple emulsions. To illustrate this, we construct a triple emulsion device, consisting of three flow-focus junctions in series. To form W/O/W/O triple emulsions, we pattern the wettability to make the first junction hydrophobic, the second hydrophilic, and the third hydrophobic. We inject water, HFE-7500, water, and HFE-7500, all with surfactants, into the first, second, third, and fourth inlets, respectively, at flow rates of 4000 μL $h^{-1}$ for the innermost phase, 3000 μL $h^{-1}$ for the first middle phase, 3000 μL $h^{-1}$ for the second middle phase, and 7500 μL $h^{-1}$ for the outermost phase. This ensures that $\{We_{in}, Ca_{out}\} > 1$ for the first two junctions and $\{We_{in}, Ca_{out}\} < 1$ for the third, so only one dripping instability is present. This creates a triple coaxial jet in the third junction, with a water jet

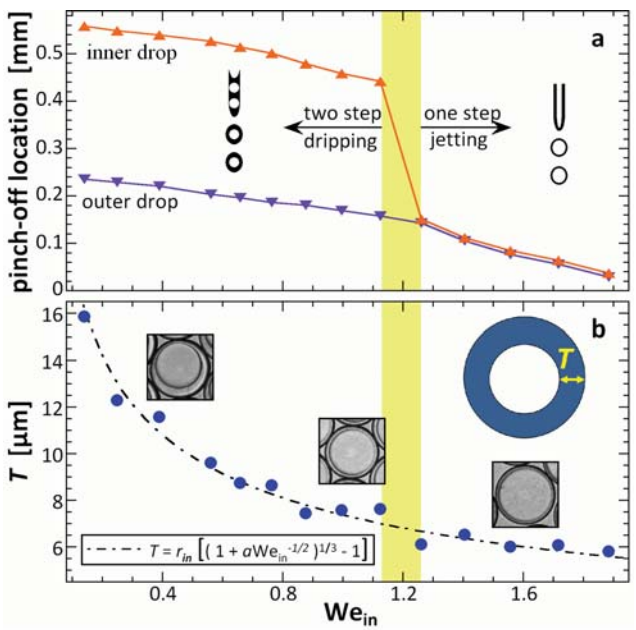


**Fig. 3** (a) Pinch-off locations of the inner and outer jets as a function of $We_{in}$. At low $We_{in}$ dripping instabilities are present in both flow-focus junctions, so the inner and outer jets break at different locations. As $We_{in}$ is increased beyond 1, the inner phase jets into the second junction; this causes the inner and outer phases to pinch off at the same place. (b) Because the first junction is not limited to the dripping regime, this allows double emulsions to be formed with thin shells. The function for $T$ is derived by equating the volume of the shell to the volume of middle phase supplied over one drop formation cycle; it is plotted by inserting the inner drop radius $r_{in}$ measured from the images, and the parameter $a = U_{mid}(\rho/\gamma l^3)^{1/2} = 0.706$, computed from known constants.

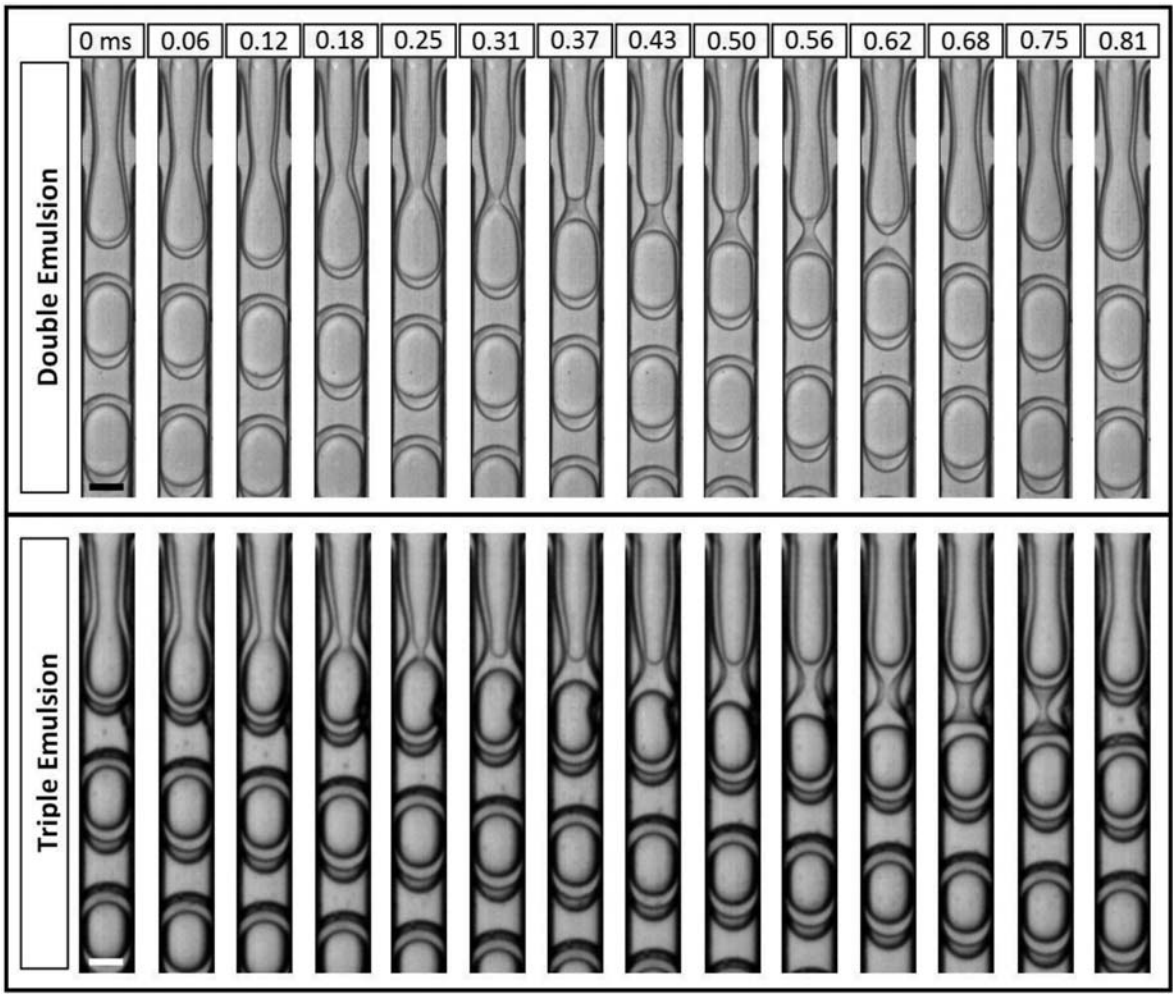


**Fig. 4** One-step formation of multiple emulsions. Double emulsions are formed by breaking a double jet, whereas triple emulsions are formed by breaking a triple jet. In these images, the inner jets break before the outer jets. As fluids for the double emulsions, we use HFE-7500 fluorocarbon oil with 1.8% of the ammonium salt of Krytox® 157 FSL (w/w) and deionized water with 0.5% SDS (w/w) as the surfactant. For the double emulsions, we inject oil, water, and oil into the first, second, and third inlets, respectively. To form triple emulsions, we inject water, oil, water, and oil into the first, second, third, and fourth inlets, respectively. The scale bar denotes 50 μm for the upper row and 80 μm for the lower row.

surrounded by an oil sheath, surrounded by another water sheath, surrounded by the oil continuous phase, as shown in Fig. 4. As with the double jet, the triple jet narrows when it enters the junction. This causes the inner jet to break, $t = 250$ μs, then the middle jet to break, $t = 625$ μs, then the outer jet to break, $t = 750$ μs, producing a triple emulsion, as shown in Fig. 4. One-step formation of this type thus consists of a series of pinching events, one for each jet as it reaches an unstable width.

A different kind of one-step formation occurs when the inner jet is more stable than the outer jet. This occurs when the innermost phase is a fluid that forms very stable jets, such as a viscoelastic fluid or a fluid with a low surface tension. To demonstrate this, we replace the innermost phase with octanol, which has a low surface tension with water, resulting in a very stable jet, and making it difficult to emulsify using microfluidic techniques. By injecting octanol as the innermost phase, we produce a coaxial jet in which the inner jet is more stable than the outer jet, Fig. 5. As the outer jet pinches into a drop, it squeezes on the inner jet, pinching it into a drop as well. This produces a double emulsion with an octanol core, as shown in Fig. 5. Because a dripping instability is used, the double emulsions are monodisperse, as are the octanol cores. In essence, this enables a difficult fluid like octanol to be controllably emulsified, and provides a new way to create emulsions from such fluids. This method can also be applied to other difficult fluids, such as viscoelastic polymer fluids. These fluids are needed when templating particles or capsules from emulsions; however, due to their viscoelastic properties, they are extremely difficult to emulsify, because their elastic response under shear resists drop formation.[31] However, by surrounding the viscoelastic jet by an oil jet, it too can be controllably emulsified. We demonstrate this using a 10 wt% solution of polyethylene glycol (PEG) (mean $M_w$ 600 000) in water; frequency dependent shear behavior was probed at room temperature using a rheometer (ARES G2, Couette geometry). The viscous and elastic part of the complex shear modulus show scaling behavior according to the Maxwell model for viscoelastic fluids in the frequency range $\omega = 0.01$–100.[32] We determined the elastic modulus to be 1.5 Pa. As the

 

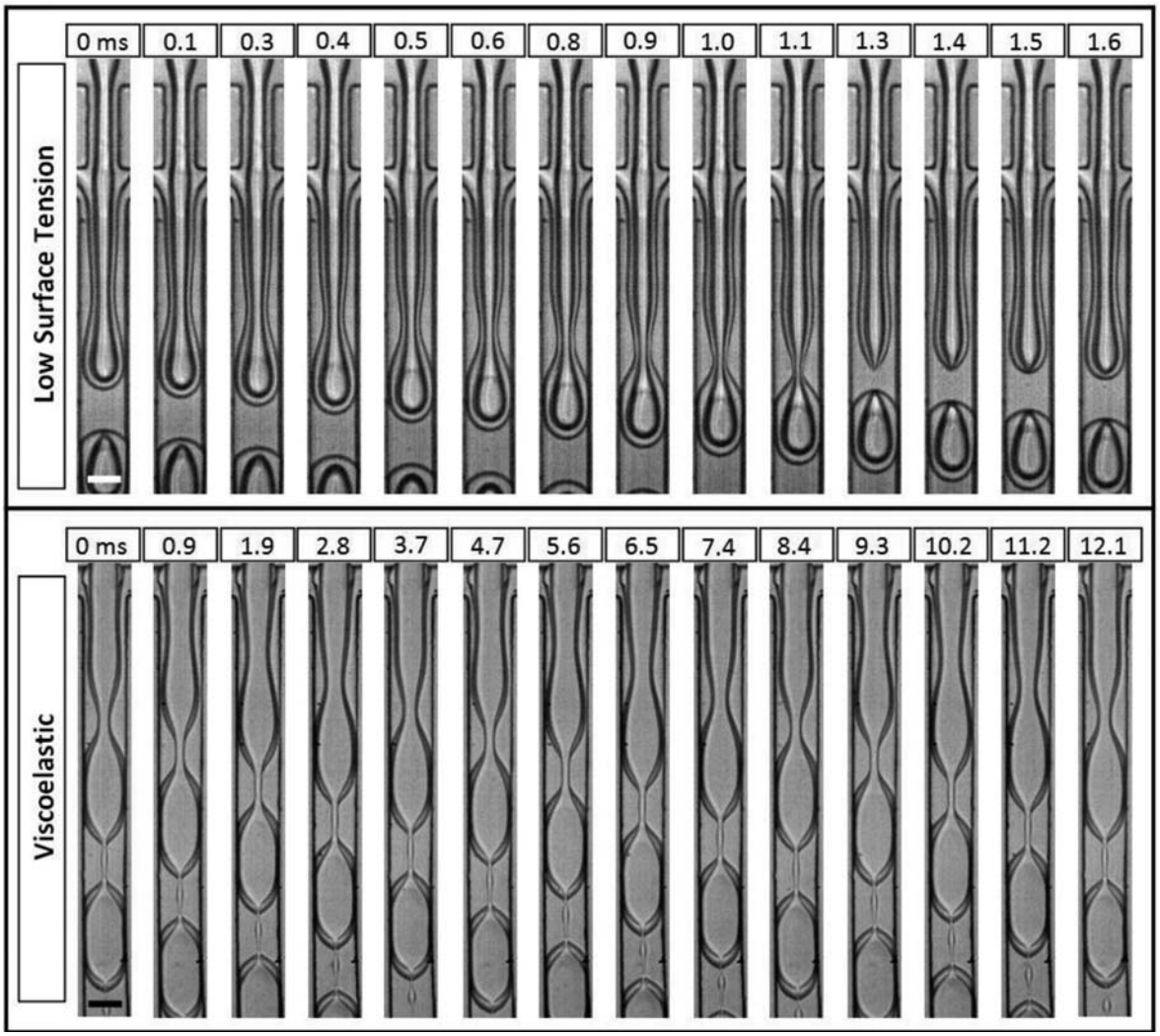


**Fig. 5** One-step formation of double emulsions in which the inner jet is composed of a fluid that does not easily break into drops. To form double emulsions from a fluid which has a very low interfacial tension with water, we inject octanol as the inner phase. To form double emulsions from a viscoelastic fluid, we inject polyethylene glycol (mean $M_w$ 600 000) in water at 10% by weight as the inner phase. In either case, HFE 7500 and water are injected as the middle and continuous phase, both with surfactants. The scale bars denote 50 μm.

outer jet pinches into a drop, it also pinches the viscoelastic jet into a drop, as shown in Fig. 5. This produces double emulsions with viscoelastic cores. The cores can be released by breaking the double emulsions, yielding a monodisperse population of viscoelastic drops.

To quantify the dynamics of these breakups, we measure the jet widths as a function of time. Early in the process the inner and outer jets narrow in unison, as shown in Fig. 6a. When the inner jet reaches an unstable width, it breaks, rapidly narrowing and forming a drop. Interestingly, this coincides with a slight widening of the outer jet, showing that additional middle-phase fluid rushes into the void left by the collapse of the inner jet, as shown in Fig. 6a. Eventually, the outer jet also collapses, forming a double emulsion. In the case of the triple emulsion, this is followed by another widening and collapse of the third jet, as shown in Fig. 6b. The functional form of the collapse for the inner and outer jets is the same and can be fit to a power law with exponent 1/2. This is consistent with the breakup of a single jet due to Rayleigh–Plateau instability. This similarity suggests that the jet breakup right at the moment of pinch-off for each of the nested jets is similar to that of a single jet.[33,34]

When the inner jet is more stable than the outer one, the pinching dynamics are different. With the octanol jet, there is a prolonged narrowing of both jets followed by a sudden collapse, as shown in Fig. 6c. The functional forms can also be fit to a power law, but with exponent 2/5. This indicates that the pinching dynamics involve interactions between the jets. With the viscoelastic jet, the collapse is much slower. There is a prolonged narrowing followed by a very slow collapse; this is due to the viscoelasticity of the inner jet, as shown in Fig. 6d. These collapses can also be fit to power laws, with exponents of 1; unlike the other jets, these jets do not accelerate close to pinch off, as shown in Fig. 6d. Thus, although one-step formation can produce monodisperse double emulsions with different fluids, the pinching dynamics depend on the fluid properties.

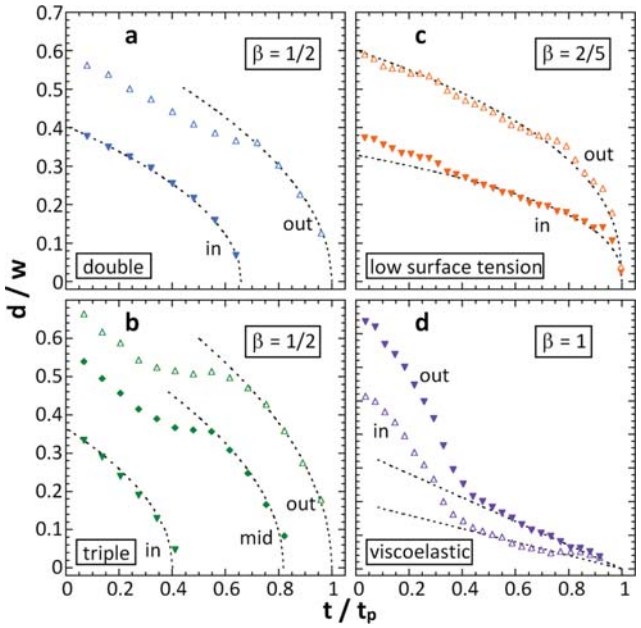


**Fig. 6** Jet diameter $d$, normalized by the channel width $w$, as a function of time during one-step formation $t$, normalized by the drop formation period $t_p$ in (a) double emulsions and (b) triple emulsions; in these cases the inner jets break before the outer jets. When the inner phase is composed of a fluid that forms stable jets, the inner and outer phases break at the same time, as they do when the inner jet (c) has a low surface tension or (d) is viscoelastic. All collapses can be fit to power laws, but with different exponents depending on the physical properties of the fluids.

## Conclusions

Microfluidic devices can form multiple emulsions in different processes by controlling dripping instabilities. If several instabilities are present, they are formed in a multi-step process, whereas if one is present, they are formed in a one-step process. The one-step process creates very thin-shelled multiple emulsions, which should be useful for capsule synthesis applications. It also enables difficult fluids, like viscoelastic fluids, to be emulsified controllably. This should be useful for synthesizing new kinds of particles requiring viscoelastic polymers.

## Acknowledgements

We thank Jim Wilking for assistance with rheological experiments and helpful discussions. This work was supported by the NSF (DMR-0602684), the Harvard MRSEC (DMR-0820484), and the Massachusetts Life Sciences Center. JT received funding from the Fund of the Chemical Industry (Germany) which is gratefully acknowledged.

## References

1 J. Bibette, F. L. Calderon and P. Poulin, *Rep. Prog. Phys.*, 1999, **62**, 969–1033.
2 A. S. Utada, E. Lorenceau, D. R. Link, P. D. Kaplan, H. A. Stone and D. A. Weitz, *Science*, 2005, **308**, 537–541.
3 A. Aserin, *Multiple Emulsion: Technology and Applications*, Wiley-VCH, 2007.
4 D. Dendukuri and P. S. Doyle, *Adv. Mater.*, 2009, **21**, 1–16.
5 M. Fujiwara, K. Shiokawa, Y. Tanaka and Y. Nakahara, *Chem. Mater.*, 2004, **16**, 5420–5426.
6 C.-H. Chen, R. K. Shah, A. R. Abate and D. A. Weitz, *Langmuir*, 2009, **25**, 4320–4323.
7 W. Engl, R. Backov and P. Panizza, *Curr. Opin. Colloid Interface Sci.*, 2007, **13**, 206–216.
8 L.-Y. Chu, A. S. Utada, R. K. Shah, J.-W. Kim and D. A. Weitz, *Angew. Chem., Int. Ed.*, 2007, **46**, 8970–8974.
9 J. Atencia and D. J. Beebe, *Nature*, 2005, **437**, 648–655.
10 E. C. Rojas, J. A. Staton, V. T. John and K. D. Papadopoulos, *Langmuir*, 2008, **24**, 7154–7160.
11 Y. D. Livney, *Curr. Opin. Colloid Interface Sci.*, 2010, **15**, 73–83.
12 M.-H. Lee, S.-G. Oh, S.-K. Moon and S.-Y. Bae, *J. Colloid Interface Sci.*, 2001, **240**, 83–89.
13 A. J. Khopade, K. S. Nandakumar and N. K. Jain, *J. Drug Targeting*, 1998, **6**, 285–292.
14 Ö. Özer, M. Özyazici, M. Tedajo, M. S. Taner and K. Köseoglu, *Drug Delivery*, 2007, **14**, 139–145.
15 G. M. S. El Shafei, M. M. El-Said, H. A. E. Attia and T. G. M. Mohammed, *Ind. Crops Prod.*, 2009, **31**, 99–106.
16 M. Seo, C. Paquet, Z. Nie, S. Xu and E. Kumacheva, *Soft Matter*, 2007, **3**, 986–992.
17 S. Okushima, T. Nisisako, T. Torii and T. Higuchi, *Langmuir*, 2004, **20**, 9905–9908.
18 A. R. Abate and D. A. Weitz, *Small*, 2009, **5**, 2030–2032.
19 S. L. Anna, N. Bontoux and H. A. Stone, *Appl. Phys. Lett.*, 2003, **82**, 364–366.
20 A. M. Gañàn-Calvo and J. M. Gordillo, *Phys. Rev. Lett.*, 2001, **87**, 274501-1–274501-4.
21 A. S. Utada, L.-Y. Chu, A. Fernandez-Nieves, D. R. Link, C. Holtze and D. A. Weitz, *MRS Bull.*, 2007, **32**, 702–708.
22 C. N. Baroud and H. Willaime, *C. R. Phys.*, 2004, **5**, 547–555.
23 A. S. Utada, A. Fernandez-Nieves, H. A. Stone and D. A. Weitz, *Phys. Rev. Lett.*, 2007, **99**, 094502-1–094502-4.
24 T. Nisisako, S. Okushima and T. Torii, *Soft Matter*, 2005, **1**, 23–27.
25 N. Pannacci, H. Bruus, D. Bartolo, I. Etchart, T. Lockhart, Y. Hennequin, H. Willaime and P. Tabeling, *Phys. Rev. Lett.*, 2008, **101**, 164502-1–164502-4.
26 V. Barbier, M. Tatoulian, H. Li, F. Arefi-Khonsari, A. Ajdari and P. Tabeling, *Langmuir*, 2006, **22**, 5230–5232.
27 A. R. Abate, J. Thiele, M. Weinhart and D. A. Weitz, *Lab Chip*, 2010, **10**, 1774–1776.
28 Y. Hong and F. Wang, *Microfluid. Nanofluid.*, 2007, **3**, 341–346.
29 C. Cramer, P. Fischer and E. J. Windhab, *Chem. Eng. Sci.*, 2004, **59**, 3045–3058.
30 A. S. Utada, A. Fernandez-Nieves, J. M. Gordillo and D. A. Weitz, *Phys. Rev. Lett.*, 2008, **100**, 014502-1–014502-4.
31 P. E. Arratia, J. P. Gollub and D. J. Durian, *Phys. Rev. E: Stat., Nonlinear, Soft Matter Phys.*, 2008, **77**, 036309-1–036309-6.
32 J. D. Ferry, *Viscoelastic Properties of Polymers*, Wiley, 3rd edn, 1980.
33 J. W. Strutt and L. Rayleigh, *Philos. Mag. (1798–1977)*, 1892, **34**, 177–180.
34 J. Eggers and E. Villermaux, *Rep. Prog. Phys.*, 2008, **71**, 036601-1–036601-79.

 